

Formation of narrow spin-wave transmission bands in lateral magnetic superlattices

Nikolay I. Polushkin

Instituto Superior Tecnico and ICEMS, Avenue Rovisco Pais 1, 1049-001 Lisbon, Portugal

(Received 24 September 2010; published 12 November 2010)

It is shown theoretically that an alternating magnetic field applied locally to a stripe periodic heterostructure with different saturation magnetizations, M_1 and M_2 , excites dipolar spin waves, which are able to propagate along the periodicity direction within a narrow frequency band ($\Delta\omega/\omega < 5\%$) in the absence of Bragg scattering. A mechanism is found for trapping the out-of-band modes inside a potential well whose formation is mediated by spin pinning at the M_1/M_2 interfaces.

DOI: [10.1103/PhysRevB.82.172405](https://doi.org/10.1103/PhysRevB.82.172405)

PACS number(s): 75.40.Gb, 75.30.Ds, 75.40.Mg

The features of collective and individual excitations in artificial crystals composed of two different materials (superlattices) are one of the central issues in solid-state physics during the past four decades. The start to this research was given by observing the energy gaps for electron transport in semiconductor superlattices.¹ The results obtained in that work have stimulated, in particular, the studies of the wave dispersion of plasmon modes in semiconductor superlattices² and layered superconductors,³ phonon modes in semiconductor superlattices (phononic crystals),⁴ and photon modes in dielectric superlattices (photonic crystals).⁵ More recently, a strong renewed interest has arisen to periodic thin-film magnetic waveguides or so-called magnonic crystals,^{6–8} which are the magnetic counterpart of the phononic and photonic crystals. Numerous theoretical and experimental efforts were concentrated to investigate different types of magnonic crystals including periodic multilayers,^{7–9} metal overlay arrays,¹⁰ micron-size grooves^{11–14} or holes⁸ etched on yttrium iron garnet films, patterned stripe arrays in permalloy films,¹⁵ width-modulated stripe waveguides,^{16,17} and lateral periodic structures composed of two different materials.^{18–20} A common purpose of these works is to prove the existence of the frequency bands that are forbidden for spin-wave (SW) propagation at the Brillouin-zone (BZ) edges $k=n\pi/\Lambda$, where k is the wave number, n are integers, and Λ is the lattice period. Typically, SW propagation in the magnonic crystals is allowed at any frequency excluding these narrow gaps. However, previous works on periodic arrays of magnetic nanowires witnessed weak mode dispersions and increased ratios of the forbidden bands to allowed ones in such structures.^{15,19,21}

Here, we demonstrate that SW propagation can drastically be modified in lateral magnetic superlattices. Our model system is a periodic array of closely packed (without any separation) alternating stripes with two different saturation magnetizations. By numerical computation of the amplitude-frequency characteristics, we show that, due to the absence of Bragg scattering, the lowest frequency band is transparent for dipolar spin waves and that its transparency is substantially higher than that of adjacent higher frequency bands. We find that the transmission bands in such lattices are narrower than the gaps between them, which is in contrast to the typical band structure of the realistic systems.²² We identify a mechanism that contributes to the narrowing of the transmission bands in our systems. This mechanism is associated with the effects of spin pinning at the lateral interfaces. The

pinning condition prevents the SW modes from their further transmission across the system with formation of a potential well in which destructive SW interference occurs. We believe that the features reported here can be of potential interest for developing band-pass magnetic filters that are incorporated into the design of signal processing microwave devices.^{7,8,10–12,14,18} Importantly, some realistic systems such as laser-patterned heterostructures of alternating stripes with saturation magnetizations of M_1 and M_2 (Refs. 23 and 24) can be considered for such applications.

It is challenging²⁵ to find a dynamic response of a M_1/M_2 heterostructure system to a local excitation of the magnetization precession by the magnetic component of an external microwave field. A key component of magnetic microwave devices is two microstrip transducers (antennas) formed on the film surface for SW excitation and detection. In the input antenna one excites an alternating current with a frequency of ω that, in turn, generates a magnetic field $h_e f(x)\cos\omega t$. In our calculation, we neglect the dependence of all the dynamic fields on the z coordinate along the stripes (Fig. 1), as their length is taken to be infinite. One can expect that the magnetic oscillations excited under the resonance²⁴ are able to propagate along the direction of periodicity. Also, we assume that the amplitude of these propagating oscillations can be measured at the distance x_0 with a small probe such as a highly focused laser beam used for Brillouin light scattering microscopy.²⁶

As the reference film, we use a 20-nm-thick Permalloy (Py) layer whose saturation magnetization, Gilbert damping constant, and gyromagnetic ratio are $4\pi M_1=10.0$ kG, $\alpha=0.007$, and $\gamma/2\pi=2.8$ GHz kOe⁻¹. It was revealed earlier²⁷ that the magnetization in Py can be locally reduced by fo-

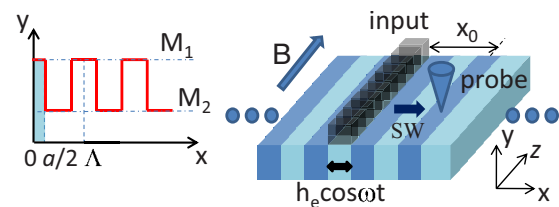


FIG. 1. (Color online) Schematic illustration, geometry of the calculation, and magnetization profile of a proposed M_1/M_2 heterostructure system. An alternating magnetic field is applied to the stripe with a magnetization of M_1 in the center of the coordinate system. The size of the excitation source is $a=\Lambda/2$.

cused ion beam. As the next step, a Py layer could be patterned with a lattice periodicity in the micron-scale regime, with formation of a periodic structure of alternating stripes with magnetizations of M_1 and M_2 . In such structures the M_1 would be equal to the saturation magnetization in the Py while the M_2 could be varied from M_1 to lower values of this quantity.

We explore how the magnetic oscillations excited locally decay along the direction of periodicity (the x axis), as shown in Fig. 1(a). An external static magnetic field B is oriented along the stripes. In this geometry the system of equations for the components of the dynamic magnetization \vec{m} with neglecting exchange can be written as

$$i\Omega 4\pi m_x(x) = -M_0(x)\langle h_y(x) \rangle_y + \Omega_H 4\pi m_y(x),$$

$$i\Omega 4\pi m_y(x) = M_0\langle h_x(x) \rangle_y - \Omega_H 4\pi m_x(x) + h_e M_0(x)f(x), \quad (1)$$

where $M_0(x)$ is the static magnetization, $\Omega = \omega/(4\pi\gamma)$, and $\Omega_H = (\gamma B + \alpha i\omega)/(4\pi\gamma)$. The dipole fields in Eq. (1) are averaged on the y coordinate and given by²⁸ $\langle h_y(x) \rangle_y = -\int_{-\infty}^{\infty} G(x, x') m_y(x') dx'$ and $\langle h_x(x) \rangle_y = -4\pi m_x(x) + \int_{-\infty}^{\infty} G(x, x') m_x(x') dx'$, where $G(x, x') = \ln[(T^2 + (x - x')^2)/(x - x')^2]$ and T is the film thickness. The components of the dynamic magnetization and external dynamic field can be represented by the Fourier integrals $m_{x(y)}(x) = (1/\sqrt{2\pi}) \int_{-\infty}^{\infty} c_{x(y)}(k) \exp(ikx) dk$ and $f(x) = (1/\sqrt{2\pi}) \int_{-\infty}^{\infty} g(k) \exp(ikx) dk$ while $M_0(x)$ is a periodic function and thus can be expanded as $M_0(x) = \sum_{n=-\infty}^{\infty} M_n \exp(iqn x)$, where $q = 2\pi/\Lambda$ and Λ is the lattice period. Substituting all these expressions into Eq. (1), multiplying the right- and left-side parts of the obtained equations by $e^{-ik'x}/(2\pi)^{1/2}$, and integrating them within the infinite limits on x , we obtain the two relations between different Fourier components of the dynamic magnetization. These relations can be reduced to the infinite system of linear algebraic equations with respect to the Fourier transform of the dynamic susceptibility $\chi(x) = 4\pi m_x(x)/h_e$

$$\sum_{j=-\infty}^{\infty} A_{jl} \chi(k - jq) = \sum_{j=-\infty}^{\infty} F_{jl} g(k - jq), \quad (2)$$

where $A_{jl} = F_{jl} - P(k - jq)D_{jl} - \lambda^2 \delta_{jl}$, $F_{jl} = D_{jl} + \Omega_H M_{j-l}$, $D_{j1} = \sum_s M_{s-l} M_{j-s} P(k - sq)$, $-\infty < s < \infty$, $\lambda^2 = \Omega^2 - \Omega_H^2$, and $P(k - jq) = \{1 - \exp[-|k - jq|T]\}/[|k - jq|T]$ are the dynamic demagnetizing factors. In a rough approximation, we assume that the external dynamic field is $f(x) = 1$ at $|x| \leq a/2$ and $f(x) = 0$ at $|x| > a/2$, so that $g(k) = (2/\pi)^{1/2} \sin(ka/2)/k$. The system in Eq. (2) was solved numerically with respect to $\chi(k)$ after cutting the number of equations to ~ 100 . Making the discrete Fourier transformation (DFT) of $\chi(k)$ in an interval from 0 to $20 \mu\text{m}^{-1}$ with a step of $0.04 \mu\text{m}^{-1}$, we retrieved the dynamic susceptibility $\chi(x)$. The accuracy of this calculation was of the order of 10%. Finally, the eigenfrequencies of the system were found by solving the secular

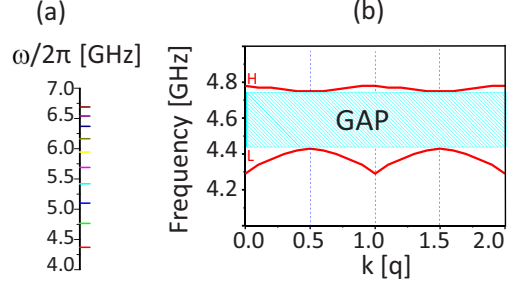


FIG. 2. (Color online) (a) Low-frequency part of the eigenvalue spectrum. Positions of the eigenfrequencies are indicated by short horizontal lines of different colors. (b) Dispersion curves within the two lowest L and H transmission bands. The gap between the transmission bands is much wider than the both of them.

equation. Their values correspond to central positions of the excitation maxima.

In Fig. 2 we show the low-frequency part of the eigenvalue spectrum (up to 10 modes) (a) and dispersion curves within the two lowest frequency excitation maxima and (b) for the lattice whose parameters chosen are as follows: $4\pi M_1 = 10.0$ kG, $4\pi M_2 = 5.0$ kG, $\Lambda = 3.0 \mu\text{m}$, and the strip-width-to-period ratio is 0.5. A chosen value of the static field B applied is 0.4 kOe. This lattice exhibits the folding zone effect,¹⁵ i.e., with changing k the mode frequencies begin to oscillate with a period of $q = 2\pi/\Lambda$. The two lowest bands noted as L and H are located at 4.37 ± 0.07 GHz and 4.765 ± 0.015 GHz, respectively. Surprisingly, the gap appearing between these two bands is much wider than the both of them. This behavior is in contrast to that occurring in other kinds of periodic systems where the band gaps are typically much narrower than those allowed for wave excitation and propagation.

All the further results reported here are obtained with an alternating magnetic field applied locally to a stripe with a larger magnetization, M_1 , so that $a = \Lambda/2$, as indicated by the blue color in Fig. 1. Figure 3 shows $\chi(k)$ [(a) and (c)] and $\chi(x)$ dependencies [(b) and (d)] within the L and H bands at the lower (4.25 and 4.72 GHz) and upper (4.45 and 4.78 GHz) band edges (red and blue curves, respectively) and near the band centers at 4.35 and 4.75 GHz (green curves). In the $\chi(k)$ dependencies we mark the presence of several maxima of the SW intensity. For instance, there are two prominent peaks at the lower edge of the L band. One of these peaks is located at the very center of the first BZ at $k = 0$, while the second one appears to be at the boundary between second and third BZ's ($k = 2\pi/\Lambda$). The peaks of SW intensity are of opposite polarity, i.e., the spin precession occurs in antiphase in them, and their contribution to the $\chi(x)$ dependence is essentially different: The low- k peak is responsible for a general decay of the SW intensity with increasing distance while the high- k peak mediate the oscillatory character of the coordinate dependence. The period of these oscillations is equal to Λ so the occurrence of the high- k peak at $k = 2\pi/\Lambda$ can easily be understood. As ω increases within the L band, the low- k peak shifts to larger k within the first BZ while the peak at $k = 2\pi/\Lambda$ splits up into the two peaks moving in the opposite directions from the BZ boundary within the second and third BZ's.

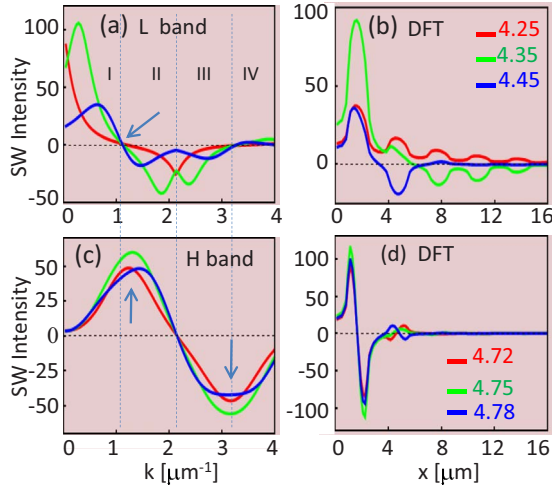


FIG. 3. (Color online) SW intensity as a function of wave number [(a) and (c)] and its DFT [(b) and (d)] within L and H bands near the lower (4.25 and 4.72 GHz) and upper (4.45 and 4.78 GHz) band edges (red and blue curves, respectively) and near band centers at 4.35 and 4.75 GHz (green curves). Arrows in (a) and (c) indicate the absence of Bragg scattering in the L band and its presence in the H band. BZ's are indicated by numbers I, II, III, and IV.

Strikingly, the $\chi(x)$ dependencies in Figs. 3(b) and 3(d) demonstrate that the transparency of the L band is substantially higher than that of the H band. One sees that in the L band the SW intensity is still persistent at $x_0 \sim 15 \mu\text{m}$ while no any SW intensity remains already at $x_0 \sim 6 \mu\text{m}$ within the H band. A reason for a higher transparency within the L band is that in this band the low- k ($k < \pi/\Lambda$) SW intensity, which mostly contributes to the rate of $\chi(x)$ decay, is smallest just near the BZ boundary and goes to zero at the very edge $k = \pi/\Lambda$, as indicated by arrow in Fig. 3(a). This means that there is no Bragg scattering in the L band and it is relatively transparent for the spin waves. Within the H band, however, the SW intensity is maximal near the BZ boundary at $k = \pi/\Lambda$. This Bragg scattering provides the loss in the SW intensity, which is indicated by the $\chi(x)$ dependencies in Fig. 3(d).

Another feature is that the SW transmission in the L -band center differs from that near its edges and, especially, near its upper edge. Practically, no any SW intensity remains at $x_0 > 7 \mu\text{m}$ near the upper edge. To find a reason for the narrowing of the transmission band in the absence of Bragg scattering, we plotted a function $|\text{Im} \chi(\omega, x_0)|$ at various x_0 . As an example, Fig. 4(a) shows this dependence normalized to the maximal value and its envelope function (red curve) at $x_0 = 7.5 \mu\text{m}$, which corresponds to the third maximum of $\text{Im} \chi(x)$. One sees from this plotting that the SW intensity is a slow function of ω near the lower edge. This is similar to that behavior taking place in a homogeneous Py layer (blue curve). However, the SW intensity alters much steeper near the upper edge where it decreases in a threshold manner at $\omega_c \approx 4.44 \text{ GHz}$. To understand such a thresholdlike behavior at $\omega \rightarrow \omega_c$, we addressed the issue of spin pinning at the M_1/M_2 interfaces. If such pinning is effective, at least, at one of the interfaces, it can provide back scattering of the spin

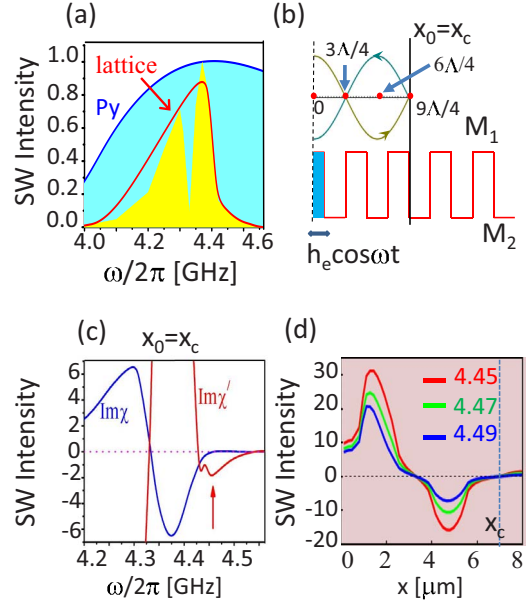


FIG. 4. (Color online) (a) $|\text{Im} \chi(\omega, x_0)|$ and its envelope function for the heterostructure system and Py layer at $x_0 = 7.5 \mu\text{m}$. (b) Simplified scheme for formation of the potential well within $|x_0| < |x_c|$ and for destructive interference of the low- k spin waves inside it. (c) Spin pinning at the interface $x_0 = x_c$ if $|\text{Im} \chi| < 0.1$ and $|\text{Im} \chi'| < 2$ at $\omega > \omega_c$. (d) Mode trapping inside the potential well at $x_0 < x_c$ and $\omega > \omega_c$. The values of ω taken for this plotting are 4.45, 4.47, and 4.49 GHz.

waves that are excited locally, within $0 < x_0 < \Lambda/2$, and travel away from the excitation source along the periodicity direction. Then, the confined volume is a potential well for such waves.²⁹ This process is shown schematically in Fig. 4(b). To find where exactly the pinning condition can fulfill in our system, we have followed how an $-\text{Im} \chi(\omega, x_0)$ function behaves at different M_1/M_2 and M_2/M_1 interfaces. Figure 4(c) shows this function and its first derivative on a dimensionless variable $\xi = 2x_0/\Lambda$ at the distance of $x_0 = 6.75 \mu\text{m}$, which corresponds to the third M_1/M_2 interface from the coordinate center ($x_c = 6.75 \mu\text{m}$). We find from this plotting that both $\text{Im} \chi$ and its derivative should *simultaneously* be small enough, $|\text{Im} \chi| < 0.1$ and $|\text{Im} \chi'(\xi)| < 2$, for formation of the potential well with effective SW reflection from its walls at $x_0 = \pm x_c$. This condition becomes valid when the frequency approaches the upper edge of the H band, as shown by arrow in Fig. 4(c). It is interesting that at $\omega = 4.334 \text{ GHz}$, where $\text{Im} \chi \rightarrow 0$ as well, the derivative is not small, $|\text{Im} \chi'(\xi)| = 3.75$.

With further increase in $\omega > \omega_c$, the SW intensity remains close to zero at any $x_0 \geq x_c$. In other words, all the out-of-band ($\omega > \omega_c$) SW modes are trapped by the $x_0 = x_c$ interface to be confined in the potential well. As seen from Fig. 4(d), no any changes in the distribution of $\chi(x)$ occur with increasing ω above the upper band edge, excluding a uniform drop in SW intensity at all distances from the excitation center. This confinement of the out-of-band modes is another result of the spin pinning at the $x_0 = x_c$ interface. In the formed potential well, the backward SW modes reflected from the interface interfere destructively with the initially excited for-

ward modes, as schematically illustrated in Fig. 4(b), resulting in the standing wave pattern with the nodes at $\pm 3\Lambda/4$ and $\pm 9\Lambda/4$. Since the period of this standing wave pattern is equal to 3Λ , such a qualitative picture is compatible with the $\chi(k)$ dependencies for the out-of-band modes whose maximal wavelengths are $2\pi/k_{\max} \sim 10 \mu\text{m}$, as seen from Fig. 3(a) (blue curve).

In summary, a possibility is shown for dipolar spin-wave transmission across a thin ferromagnetic layer with periodic modulation of the saturation magnetization along a lateral direction. In such superlattices the spin waves propagate

within a narrow lowest frequency band, whose width is strongly limited by the pinning condition at the lateral interfaces. All the other (higher frequency) bands are not transparent for spin-wave propagation. The obtained results open a new room for the studies of periodic magnetic systems in the light of their applicability to signal processing microwave devices.

Work was supported by the program ‘‘Ciencia 2008’’ funded by the Portugal Foundation of Science and Technology.

-
- ¹L. Esaki, in *Novel Materials and Techniques in Condensed Matter*, edited by G. W. Crabtree and P. Vashishta (North-Holland, New York, 1982), p. 1.
- ²G. F. Giuliani and J. J. Quinn, *Phys. Rev. Lett.* **51**, 919 (1983).
- ³H. A. Fertig and S. Das Sarma, *Phys. Rev. Lett.* **65**, 1482 (1990).
- ⁴M. S. Kushwaha, P. Halevi, L. Dobrzynski, and B. Djafari-Rouhani, *Phys. Rev. Lett.* **71**, 2022 (1993).
- ⁵E. Yablonovitch, *Phys. Rev. Lett.* **58**, 2059 (1987).
- ⁶J. O. Vasseur, L. Dobrzynski, B. Djafari-Rouhani, and H. Puzkarski, *Phys. Rev. B* **54**, 1043 (1996).
- ⁷S. A. Nikitov, Ph. Tailhades, and C. S. Tsai, *J. Magn. Magn. Mater.* **236**, 320 (2001).
- ⁸Y. V. Gulyaev *et al.*, *JETP Lett.* **77**, 567 (2003).
- ⁹V. V. Kruglyak *et al.*, *J. Appl. Phys.* **98**, 014304 (2005).
- ¹⁰J. M. Owens *et al.*, *IEEE Trans. Magn.* **14**, 820 (1978).
- ¹¹C. G. Sykes, J. D. Adam, and J. H. Collins, *Appl. Phys. Lett.* **29**, 388 (1976).
- ¹²J. P. Parekh and H. S. Tuan, *Appl. Phys. Lett.* **30**, 667 (1977).
- ¹³A. V. Chumak *et al.*, *Appl. Phys. Lett.* **94**, 172511 (2009).
- ¹⁴A. B. Ustinov, A. V. Drozdovskii, and B. A. Kalinikos, *Appl. Phys. Lett.* **96**, 142513 (2010).
- ¹⁵G. Gubbiotti, S. Tacchi, G. Carlotti, P. Vavassori, N. Singh, S. Goolaup, A. O. Adeyeye, A. Stashkevich, and M. Kostylev, *Phys. Rev. B* **72**, 224413 (2005); *Appl. Phys. Lett.* **90**, 092503 (2007).
- ¹⁶K.-S. Lee, D.-S. Han, and S.-K. Kim, *Phys. Rev. Lett.* **102**, 127202 (2009); *Appl. Phys. Lett.* **95**, 082507 (2009).
- ¹⁷A. V. Chumak *et al.*, *Appl. Phys. Lett.* **95**, 262508 (2009).
- ¹⁸R. L. Carter *et al.*, *J. Appl. Phys.* **53**, 2655 (1982).
- ¹⁹Z. K. Wang *et al.*, *Appl. Phys. Lett.* **94**, 083112 (2009).
- ²⁰D. S. Deng, X. F. Jin, and R. Tao, *Phys. Rev. B* **66**, 104435 (2002).
- ²¹J. Topp, D. Heitmann, M. P. Kostylev, and D. Grundler, *Phys. Rev. Lett.* **104**, 207205 (2010).
- ²²One example of the system with large gaps is given by H. Al-Wahsh, A. Akjouj, B. Djafari-Rouhani, J. O. Vasseur, L. Dobrzynski, and P. A. Deymier, *Phys. Rev. B* **59**, 8709 (1999).
- ²³N. I. Polushkin, S. A. Michalski, L. Yue, and R. D. Kirby, *Phys. Rev. Lett.* **97**, 256401 (2006).
- ²⁴N. I. Polushkin, *Phys. Rev. B* **77**, 180401(R) (2008).
- ²⁵R. Hertel, W. Wulfhekel, and J. Kirschner, *Phys. Rev. Lett.* **93**, 257202 (2004).
- ²⁶V. E. Demidov *et al.*, *Appl. Phys. Lett.* **92**, 232503 (2008).
- ²⁷L. Folks *et al.*, *J. Phys. D: Appl. Phys.* **36**, 2601 (2003).
- ²⁸K. Y. Guslienko, S. O. Demokritov, B. Hillebrands, and A. N. Slavin, *Phys. Rev. B* **66**, 132402 (2002).
- ²⁹C. F. Kooi *et al.*, *J. Appl. Phys.* **35**, 791 (1964).